September 20-23, 2011
City of Cuernavaca México
XI International
Hydrogen Congress
an event of The Mexican Hydrogen Society
Cuernavaca...
The Endless Spring

ABSORPTION ENHANCED REFORMING OF LIGHT ALCOHOLS (METHANOL AND ETHANOL) FOR THE PRODUCTION OF HYDROGEN: THERMODYNAMIC MODELING

Miguel A. Escobedo Bretado[1], Manuel D. Delgado Vigil[2], Jesús Salinas Gutiérrez[2], Miguel Meléndez Zaragoza[2], Virginia Collins-Martínez[2] and Alejandro López Ortiz[2]

[1] Facultad de Ciencias Químicas, Universidad Juárez del Estado de Durango, Ave. Veterinaria s/n, Circuito Universitario, Durango 34120, México
[2] Departamento de Materiales Nanoestructurados, Centro de Investigación en Materiales Avanzados, S.C. Miguel de Cervantes 120, Chihuahua, Chih. 31109, México,
* contact email: alejandro.lopez@cimav.edu.mx

ABSTRACT

Thermodynamic modeling of the steam reforming of light alcohols using CaO, CaO*MgO, Na_2ZrO_3, Li_2ZrO_3 and Li_4SiO_4 as CO_2 absorbents was carried out to determine promising operating conditions to produce a high hydrogen production ratio (HR) and concentration (% H_2) gas product. Light alcohols studied were ethanol and methanol at 300-850°C and 1 atm. Steam to alcohol (S/COH) molar feed ratio varied from 1:1 (stoichiometric) to 6:1 for methanol and from 3:1 (stoichiometric) to 6:1 for ethanol. Thermodynamic simulation employed the Gibbs free energy minimization technique to obtain equilibrium compositions. Results indicate no carbon formation at S/COH ≤ stoichiometric. Methanol reforming at 600°C and S/COH = 6, without CO_2 absorbent (WOA), produced a hydrogen ratio (HR) of 2.76 (molsH_2/molCH_3OH fed) and 73.5% H_2. At the same conditions CaO, CaO*MgO, and Na_2ZrO_3 produced a HR (% H_2) of 2.98 (98.2% H_2), 2.96 (96.4% H_2) and 2.91 (98.2% H_2), respectively. Ethanol reforming WOA generated a HR = 4.6 (69.5% H_2) at 600°C and S/COH = 6, while CaO, CaO*MgO, and Na_2ZrO_3 showed a HR (% H_2) of 5.7 (96.6% H_2), 5.5 (94.1% H_2) and 5.4 (92.3% H_2), respectively. For both cases other absorbents produced lower values. In both reforming systems (methanol and ethanol) most favorable thermodynamics were obtained with CaO and CaO*MgO as absorbents; however stability of these absorbents CaO*MgO, and Na_2ZrO_3 must be improved. While, Na_2ZrO_3 is a promising alternate absorbent with comparable thermodynamics and greater kinetics and stability. Modeling results agreed with experimental evaluation of ethanol reforming using CaO*MgO, and Na_2ZrO_3.

Key words: Absorption-Enhanced-Reforming, Ethanol, Methanol, CO_2 absorbent, Thermodynamics

1. INTRODUCTION

Today, fossil fuel reserves are in the way of depletion, since crude oil (a non-renewable resource), cannot continue to meet the ongoing demand. Particularly, oil production has become limited by the current capacity of extraction technology, causing supply and demand curves to diverge. Therefore, the age of cheap liquid fuels is coming to an end, and a condition of meeting additional demand is to develop unconventional resources, which translates to an increase in the price of petroleum products. Furthermore, the capacity to meet liquid fuel demand is depending upon the fast and immediate diversification of liquid fuels, the transition to alternative energy carriers where applicable, and demand side measures such as behavioral change and adaptation. [1]. Two main important issues are considered in the fossil fuel substitution; clean and environmentally friendly fuels and improve their efficiency in energy conversion. In recent years, fuel cells have become an option for high efficiency power generation based on renewable hydrogen.

Hydrogen is an important raw material in the chemical and petroleum industries. Moreover, hydrogen might become a new generation of clean energy carrier for transport, especially for fuel cell applications, which would cause a huge increase in the hydrogen demand. Today 95% of hydrogen production is based on the steam reforming of natural gas [2]. However, there is an expected increase in hydrogen demand that is related to fuel cell applications, which could drive the development of new methods for its production, particularly from renewable sources. The use of biofuels (ethanol, diesel, etc.) for hydrogen production, through conventional industrial processes (steam reforming, partial oxidation and dry reforming), presents the advantage of a zero CO_2 balance during the biofuels conversion, since the carbon dioxide released to the atmosphere can be absorbed during the biomass formation process [3]. Ethanol and methanol are considered potential candidates for hydrogen production from biomass [4]. Bio-ethanol can be obtained from different biomass sources, which include; energy crops, agro industrial wastes, organic material from urban solid wastes, etc. On the other hand, bio-methanol as a second generation biofuel can also be considered as a suitable feedstock for hydrogen production.

Methanol is conventionally produced from fossil natural gas or by coal gasification, while biomethanol is made from biogas generated exclusively from renewable and non-food crop resources [5].

It is important to state that from these two potential fuels (ethanol and methanol) methanol presents the highest value in hydrogen/carbon (H/C) atomic ratio and this means that in principle its conversion could lead to a high purity hydrogen stream with expected low carbon formation.

Otherwise, the steam reforming of ethanol and/or methanol, which are oxygenated hydrocarbons, is rather thermodynamically favored at lower temperatures than non oxygenated hydrocarbons such as methane [6]. Steam reforming of methanol and ethanol for hydrogen production follow the next stoichiometric reactions:

$$CH_3OH(g) + H_2O(g) = CO_2(g) + 3H_2(g) \qquad \Delta H°_{298} = 48.2 \text{ kJ/mol} \qquad (1)$$

$$C_2H_6O(g) + 3H_2O(g) = 2CO_2(g) + 6H_2(g) \qquad \Delta H°_{298} = 171.2 \text{ kJ/mol} \qquad (2)$$

Even though these reactions appear to be simple, these are accompanied with a complex reaction system of undesired reaction paths. Therefore, the hydrogen selectivity is dictated and limited by the thermodynamic equilibrium of the reaction system. For proton exchange membrane fuel cell (PEMFC) applications the maximum hydrogen production can be carried out in three steps. The first step is the conversion of the biofuel into H_2, CH_4, CO and CO_2 (steam reforming) followed by a low temperature step where most of the CO produced is converted in CO_2 and additional H_2 by the water gas shift reaction (WGS):

.

$$CO(g) + H_2O(g) = CO_2(g) + H_2(g) \qquad \Delta H°_{298} = -41.2 \text{ kJ/mol} \qquad (3)$$

Since the WGS is limited by the thermodynamic equilibrium the CO concentration after this step *is still high to be used in the PEMFC anode where a CO concentration greater than 50 ppm will*

cause poisoning of the platinum catalyst. Consequently, a third step should be carried out, which consists to remove the carbon monoxide such as preferential oxidation (polishing step). Finally, in order to generate electric energy, the high purity hydrogen produced and oxygen can be used as a feedstock for a PEMFC.

The need for a high purity hydrogen stream for PEMFC applications, without the need of a process of several steps that conventional processes currently employ, has led to the scientific community to propose alternate processes such as the absorption enhanced reforming (AER). This AER process provides a promising alternative for a single step high purity hydrogen production [7]. The fundamental concept in which this process is based is the Le Chatellier's principle in which the reaction equilibrium can be shifted towards the production of hydrogen when CO_2 is removed *in situ* within the reforming reactor. Thus if the carbon dioxide generated during the steam reforming step is removed from the gas phase using a solid CO_2 absorbent such as CaO the hydrogen production will be enhanced. In the AER reactor a mixture of a CO_2 absorbent (for example CaO) and a reforming catalyst will theoretically produce a high purity hydrogen stream in one single step. The combination of the CO_2 absorption by CaO through the reaction:

$$CaO + CO_2(g) = CaCO_3 \qquad \Delta H°_{298} = -178.3 \text{ kJ/mol} \tag{4}$$

and the steam reforming of methanol and ethanol lead to the following reactions:

$$CH_3OH(g) + H_2O(g) + CaO = CaCO_3 + 3H_2(g) \qquad \Delta H°_{298} = -130 \text{ kJ/mol} \tag{5}$$

$$C_2H_6O(g) + 3H_2O(g) + 2CaO = 2CaCO_3 + 6H_2(g) \qquad \Delta H°_{298} = -185.3 \text{ kJ/mol} \tag{6}$$

Comparing equations (1) and (2) with equations (5) and (6), it is evident that the use of a CO_2 absorbent change from endothermic steam reforming reactions to exothermic reactions, which implies potential energy savings with the use of both biofuels. However, this absorbent must be

regenerated if a continuous process is desired and then the high endothermic reverse reaction (4) will eventually be required to be performed.

Thermodynamic analyses and experimental studies related to the use of simultaneous CO_2 removal using CaO as absorbent combined with the steam reforming of methanol and/or ethanol for hydrogen production has been reported by several authors [8, 9]. However, calcium-base absorbents lose more than half of their absorption capacity after several absorption/regeneration cycles (typically five), with the exception of calcined dolomite (CaO*MgO) which is able to withstand several cycles with minor deterioration. The loss of capacity in these absorbents is due to sintering of the materials consequence of the high temperature required for their regeneration (T > 900°C) [10]. Therefore, the use of a suitable absorbent that combines relatively low regeneration temperatures and good multicycle performance is highly desirable.

Recent studies have developed synthetic CO_2 absorbents. Compounds such as: lithium orthosilicate (Li_4SiO_4), lithium zirconate (Li_2ZrO_3) [11] and sodium zirconate (Na_2ZrO_3) [12], which are able to withstand many carbonation/regeneration cycles without important loss of CO_2 absorption capacity and activity at high temperatures. Therefore, these synthetic absorbents have become potential candidates to be used under the proposed AER process.

In the present study, a thermodynamic analysis of steam reforming of two light alcohols, methanol and ethanol, with and without the use of a CO_2 absorbent was carried out to determine favorable operating conditions to produce a high purity hydrogen stream suitable for PEMFC applications. The CO_2 absorbents studied were; CaO, CaO*MgO, Na_2ZrO_3, Li_2ZrO_3 and Li_4SiO_4. The influence of steam-to-fuel feed molar ratio and temperature on the product gas concentration was investigated for all cases. Also, in the AER reaction system, pressure was kept at atmospheric conditions. Results are compared with experimental (where available) and theoretical data generated and found in existing literature. Furthermore, it is expected that during the steam reforming of alcohols, carbon deposition over catalysts may be the main cause for deactivation, resulting in low durability and activity loss. Therefore, additionally a study of

conditions where this carbon deposition is expected with and without the use of a CO_2 absorbent is presented. Finally, the thermal efficiency is evaluated in the conventional steam reforming and AER processes for each absorbent studied.

2. SIMULATION CALCULATIONS

2.1 Gibbs Free Energy Minimization Technique

In a reaction system where many simultaneous reactions take place, equilibrium calculations can be performed through the Gibbs energy minimization approach (also called the non stoichiometric method). In this technique the total free energy of the system consisting of an ideal gas phase and pure condensed phases, can be expressed as:

$$\frac{G}{RT} = \left\{ \sum_{i=1}^{N} n_i \frac{G_i^{\circ}}{RT} + \ln\,(y_i P) \right\}_{gas} + \frac{1}{RT} \left\{ \sum_{i=1}^{N} n_i\, G_i^{\circ} \right\}_{condensed} \qquad (7)$$

The technique is based in finding different values of n_i which minimizes the objective function (7) and subjected to the constraints of the elemental mass balance:

$$\sum_{i=1}^{N} a_{ij}\, n_i = A_j, \quad j = 1, 2, 3 \ldots, k \qquad (8)$$

where a_{ij} is the number of atoms of the j^{th} element in a mole of the i^{th} species. A_j is defined as the total number of atoms of the j^{th} element in the reaction mixture [13]. All calculations were performed through the using the equilibrium module of the HSC chemistry software for windows [14]. HSC calculates the equilibrium composition of all possible combination of reactions that are able to take place within the thermodynamic system. These equilibrium calculations make use of the equilibrium composition module of the HSC program that is based on the Gibbs free energy minimization technique. The GIBBS program of this module finds the most stable phase combination and seeks the phase compositions where the Gibbs free energy of the system reaches

its minimum (equation 7) at a fixed mass balance (a constraint minimization problem, equation 8), constant pressure and temperature.

In this non-stoichiometric approach every species in the system must be defined. The selection of feasible products should be based on previous experimental results found in the literature. For each system the possible species are specified based on reported experimental and thermodynamic analysis studies. In the methanol and ethanol steam reforming system the species included were: ethanol, ethylene, ethane, acetone, acetaldehyde, acetic acid, C, CO, CH_4, CO_2, H_2, and H_2O and these were based on reported experimental species found in the literature [15-17]. Identical conditions were used for the cases where a CO_2 absorbent was included, with the exception that two solid phases were added; solid and elemental carbon. In the case of CO_2 absorbent CaO, the species $Ca(OH)_2$ and $CaCO_3$ were added. For dolomite were: CaO*MgO, CaO, $CaCO_3$, $MgCO_3$ and MgO. For sodium zirconate were: Na_2ZrO_3, Na_2CO_3 and ZrO_2. For lithium zirconate were: Li_2ZrO_3, Li_2CO_3 and ZrO_2 and finally for lithium orthosilicate were: Li_4SiO_4, Li_2CO_3 and Li_2SiO_3 all of these correspond to the following carbonation reactions:

$$CaO*MgO + CO_2(g) = CaCO_3 + MgO \qquad \Delta H°_{298} = -170.9 \text{ kJ/mol} \qquad (9)$$

$$Na_2ZrO_3 + CO_2(g) = Na_2CO_3 + ZrO_2 \qquad \Delta H°_{298} = -151.5 \text{ kJ/mol} \qquad (10)$$

$$Li_2ZrO_3 + CO_2(g) = Li_2CO_3 + ZrO_2 \qquad \Delta H°_{298} = -162.5 \text{ kJ/mol} \qquad (11)$$

$$Li_4SiO_4 + CO_2(g) = Li_2CO_3 + Li_2SiO_3 \qquad \Delta H°_{298} = -142.2 \text{ kJ/mol} \qquad (12)$$

During the simulation work the reaction temperature was varied in the range of 300-850°C at 1 atm. Steam to alcohol (S/COH) molar feed ratio varied from 1:1 (stoichiometric) to 1:6 for methanol and from 1:3 (stoichiometric) to 1:6 for ethanol. For the case of the carbon formation study the S/COH molar feed ratio varied from 0.2 to 0.5 for each biofuel.

2.2 Thermal Efficiency Calculation

In the present work, the calculation procedure for thermal efficiency was based on the approach developed by He and coworkers [18]. For converting a fuel into hydrogen by means of the conventional steam reforming (SR) process, the efficiency of the reaction can be calculated by the following expression:

$$\eta_{SR}(\%) = \frac{n_{H_2}^{out}\ LHV_{H_2}}{\left[n_{fuel}^{in} LHV_{fuel} + Q_{input,SR} + n_{steam}^{in} \Delta H_{latent}\right]} * 100 \qquad (13)$$

where $n_{H_2}^{out}$ is the number of moles of H_2 in the outlet stream calculated at equilibrium conditions, n_{fuel}^{in} and n_{steam}^{in} are the number of moles in the inlet stream of fuel and steam, respectively, ΔH_{latent} is the latent energy of steam fed, and LHV_{H_2} and LHV_{fuel} are the lower heating values of hydrogen and fuel, respectively. The calculated values for the LHV of hydrogen, ethanol and methanol are 239.2, 1240, and 651.7 kJ/mol, respectively. According to equations (1) and (2) the maximum thermal efficiency for converting a biofuel with steam can be found by assuming that one mol of fuel produce 3 and 6 moles of H_2, for methanol and ethanol, respectively. And this is true if only the reforming reaction may take place in the system. However, it has to be considered that each reaction system is thermodynamically limited and therefore a complex network of reactions occur in this leading to a non-trivial equilibrium composition that will eventually dictate the thermal efficiency of the reaction system. Otherwise, the equilibrium composition and energy requirements depend on reaction conditions. Thus, the energy input in the reaction system, $Q_{input,SR}$ can be calculated as the enthalpy change due to the conversion of the fuel in other words, the heat duty of the reaction system:

$$Q_{input,SR} = H_{out,T} - H_{in,T} = \Delta H_{SR} \qquad (14)$$

where $H_{out,T}$ and $H_{in,T}$ are the outlet and inlet enthalpies, respectively. The GIBBS module of the HSC equilibrium performs such calculation as reaction enthalpy, ΔH_{SR}.

For the AER system the procedure to calculate the thermal efficiency is similar to the one described above for the conventional SR process. However, the energy input in the AER process, $Q_{input,AER}$ takes into account both the enthalpy change due to the fuel and the CO_2 absorbent conversion (ΔH_{AER} reaction enthalpy in HSC) and the heat required for regenerating the absorbent (ΔH_{reg}). In fact, in order to obtain a continuous and economically feasible process, the CO_2 absorbent has to be recycled through carbonation/decarbonation reactions. The energy required to regenerate the carbonated absorbents is dictated by the ΔH of regeneration reverse reactions (4), and (9) through (12) at the required temperature. Therefore the $Q_{input,AER}$ can be determined as follows:

$$Q_{input,AER} = \Delta H_{AER} + \Delta H_{Reg} \qquad (15)$$

For all the absorbents studied the ΔH_{Reg} can be calculated at specific regeneration temperatures. Furthermore, in ΔH_{AER} calculation HSC takes into account the fact that the feed to the reactor is composed by biofuel, steam and a solid CO_2 absorbent (typically 50% excess). Then the efficiency of the AER process can be estimated as follows:

$$\eta_{SR}(\%) = \frac{n_{H_2}^{out}\ LHV_{H_2}}{\left[n_{fuel}^{in} LHV_{fuel} + Q_{input,AER} + n_{steam}^{in} \Delta H_{latent}\right]} * 100 \qquad (16)$$

Therefore, the thermal efficiency depends on the production of hydrogen and the required consumption of heat (heat duty) employed to regenerate the solid CO_2 absorbent.

All the previous description of the simulation calculations is based on theoretical thermodynamic considerations and these are to be taken as a guide to further experimental evaluation of the reaction systems, since no heat and mass diffusional limitations as well as kinetics effects were taken into account for the conformation of the present thermodynamic analysis.

3. RESULTS AND DISCUSSION

3.1 Thermodynamically Possible Products

During the equilibrium calculations the HSC program requires the input of all possible chemical species present in the system as reactants and products. For the steam reforming system with and without absorbents the species considered at equilibrium were all gaseous and solid species already described in section 2.1 and the ones that were found in the current literature that appear when each biofuel is converted along with other intermediate oxygenated hydrocarbons. For the ethanol reforming system the additional intermediate species considered were: ethylene, ethane, acetaldehyde, acetic acid and acetone [8, 9, 19-21]. Whereas, for the methanol steam reforming no additional compounds were included in the calculations, since no other species were reported as additional byproducts in the literature. In practice alcohol steam reforming reactions are under kinetic control, where suitable catalysts and supports are able to completely convert all the biofuels to avoid intermediate products. All this agrees well with the fact that only trace amounts (less than 1ppm) of these oxygenated intermediates were found in all the thermodynamic calculations performed and therefore these were not reported in the present study.

3.2 Ethanol Steam Reforming System

Figure 1 presents the effects of temperature, steam to ethanol molar feed ratio (S/EtOH) on hydrogen production ratio (HR, defined as mols of H_2 produced at equilibrium per mols of ethanol fed to the system) and H_2 dry basis gas concentration (% H_2) in the product. This HR is a way to quantitatively compare different reactions systems (with and without a CO_2 absorbent) for the hydrogen production at equilibrium.

The S/EtOH was varied from 3:1 (stoichiometric) to 6:1 in a temperature range of 300-900°C. In this conventional system the production of CO (not shown in Figure) and H_2 are grown as temperature increases, since low temperatures corresponds with low CO and H_2 production (as low as 10% H_2 at 300°C). At these (low T = 300°C) same conditions CO_2 (25%) and CH_4 (66%) are the predominant gaseous species.

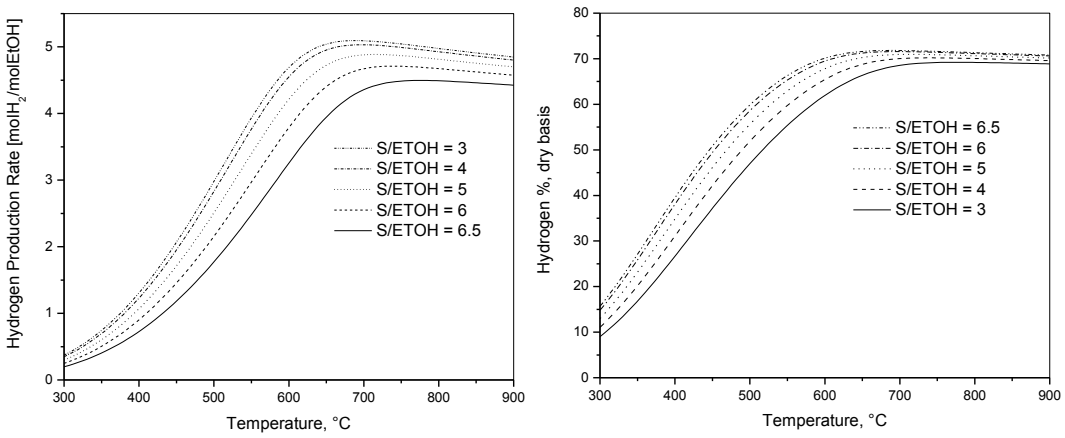

Figure 1. Equilibrium HR and H_2 for Ethanol Steam Reforming.

These results can be explained by the following methanation reactions:

$$2CO(g) + 2H_2(g) = CH_4(g) + CO_2(g) \qquad \Delta H°_{298} = -247.4 \text{ kJ/mol} \qquad (17)$$

$$CO_2(g) + 4H_2(g) = CH_4(g) + 2H_2O(g) \qquad \Delta H°_{298} = -169.9 \text{ kJ/mol} \qquad (19)$$

$$CO(g) + 3H_2(g) = CH_4(g) + H_2O(g) \qquad \Delta H°_{298} = -206.2 \text{ kJ/mol} \qquad (20)$$

$$C(s) + 2H_2(g) = CH_4(g) \qquad \Delta H°_{298} = -74.8 \text{ kJ/mol} \qquad (21)$$

Here, all the CO and H_2 produced are almost consumed by reactions (17)-(21) with the consequent generation of methane and CO_2 as the main gas products.

From Figure 1 it is evident that the hydrogen production ratio and composition are strongly enhanced with the increase of temperature. Here the higher the S/EtOH, the higher the HR and $\%H_2$ concentration. The locus of maximum HR is between 600-700°C, since there is a clear difference in HR from S/EtOH = 3 (4.4) to 9 (4.9). Higher vales than S/EtOH = 6, only increased the HR marginally, since S/EtOH = 6 produced HR of 5.0 and S/EtOH = 6.5 of 5.1. Also, it is important to notice that a greater amount of hydrogen is produced as the S/EtOH increased towards lower temperatures. This is not obvious in the case of the H_2 concentration plot (right), since the H_2 concentration increases from 62.9% at S/EtOH = 3 to 70.5% at S/EtOH = 6.5 at at

about 650°C and from there remains as plateau for all S/EtOH ratios. This plateau in H_2 concentration can be explained in terms of the inhibition of the exothermic WGS reaction (3). Furthermore, at higher temperatures the methane concentration decreases from 66% at 350°C to about 1.5% at 700°C for S/EtOH = 3, while CO_2 concentration also decreases gradually from 25 to 10.5% at the same conditions. At the same time, CO concentration increases continuously with temperature from 0.042 to 19.6% from 300-700°C. This behavior can be attributed to the reverse WGS reaction. The above described trends are consistent with previous thermodynamic analysis of this system performed by Fishtik et al. and Lima da Silva and Müller [8, 22]. These authors claim that methane dry reforming (reverse reaction 17) and steam reforming (reverse reactions 19 and 20) domain at temperatures greater than 550°C. Also, this is in agreement with experimental findings of Li et al. [23] who reported the effect of temperature on the product gas composition for the ethanol steam reforming over a $NiMg_6$ catalyst for a S/EtOH = 6. Since, as temperature was increased from 450 to 700°C they observed a gradual decrease in CO_2 and CH_4 concentrations, while CO and H_2 increased in this range. The present study generated a CO and H_2 concentrations of 1.27 and 49.7% at 450°C to 12.61 and 71.6% at 700°C, respectively, while CO_2 and CH_4 concentrations varied from 24.04 to 15.5 and 24.9 to 0.28 mol%. These former values are very close to those observed by Li et al. and others [21, 23-25]. Therefore, it can be concluded that their experiments were not kinetically limited, since all equilibrium compositions were almost reached and that the present thermodynamic analysis can be validated with the observed experimental reported values.

3.2.1 AER of Ethanol CaO Absorbent

In the AER using the CaO absorbent the hydrogen concentration is evidently enhanced as can be seen in Figure 2. The locus of maximum HR varies from 4.86 at 728°C and S/EtOH = 3 to 5.73 at 634°C and S/EtOH = 6.5, again here it can be seen a great difference in HR as the S/EtOH increased from 3 to 6, with only a marginal increase at 6.5. While only a maximum HR of 5.08 can be achieved in the system of ethanol reforming without absorbent, which represents 12.7% less than with the use of CaO as CO_2 absorbent.

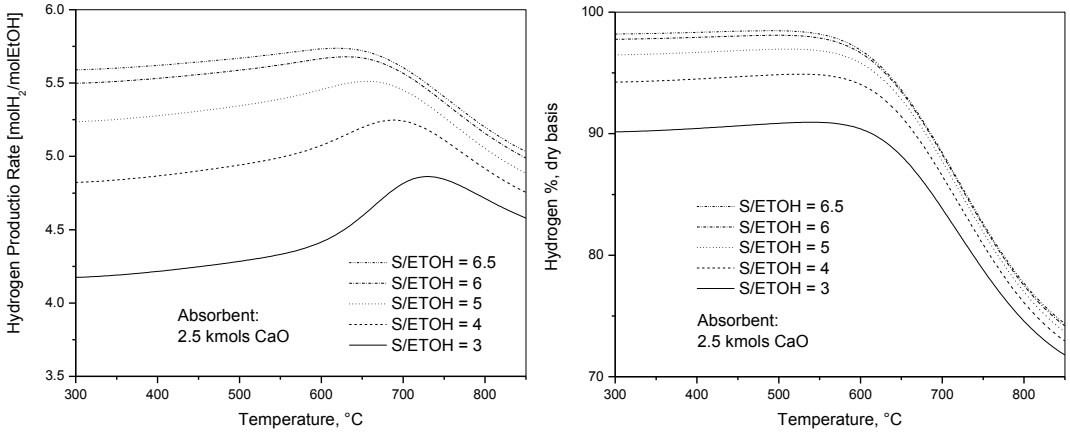

Figure 2. Equilibrium HR and H_2 for Ethanol Steam Reforming with CaO.

Also in Figure 2 the dry basis hydrogen concentration is plotted as a function of temperature and S/EtOH ratio. Here it can be seen that an almost constant plateau in H_2 concentration is achieved at low temperatures (300-600°C) and this concentration is increased as the S/EtOH also increase. The H_2 concentration at 550°C varied from 90.9% at S/EtOH = 3 to 98.2% at S/EtOH = 6.5. Greater temperature values than ≈ 600°C will eventually decrease the hydrogen % in the product gas. This can be attributed to the decrease of the ability of the CaO absorbent to capture CO_2 at high temperatures at the corresponding CO_2 partial pressure, since the carbonation reaction (4) is highly exothermic, which indicates that the CO_2 separation from the gas phase is inhibited at high temperatures. Also in this Figure it can be observed that S/EtOH values greater than 6 do not represent a significant increase in HR as well as in $\%H_2$ content. This means that a limit of S/EtOH = 6 may play a significant role in determining if greater S/EtOH values would represent an economical benefit (higher HR) compared to the cost of steam generation.

Figure 3 presents CO_2 and CH_4 concentrations as a function of temperature and S/EtOH ratio. Carbon dioxide concentrations are almost negligible at temperatures below 500°C. Greater temperature values resulted in increased CO_2 concentrations as high as 10.4% at 800°C and S/EtOH = 3, while at the same temperature a 5.6% CO_2 with S/EtOH = 6.5 can be achieved.

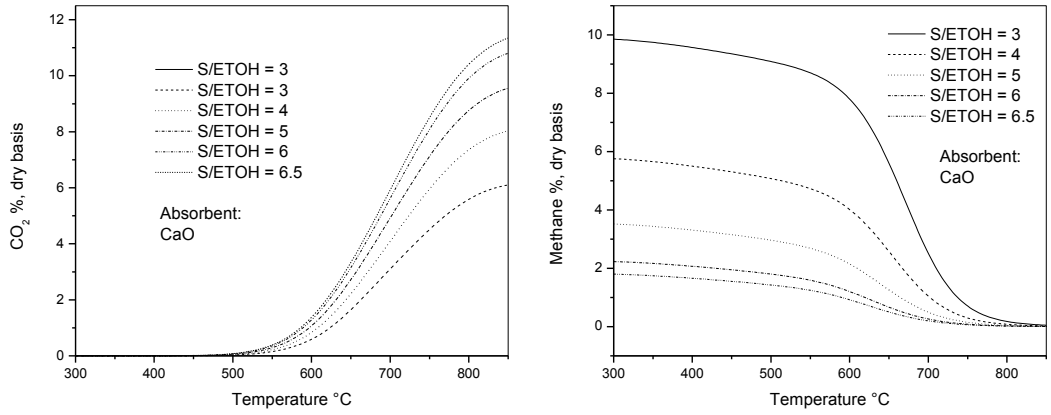

Figure 3. Equilibrium CO_2 and CH_4 compositions for Ethanol Steam Reforming with CaO

This behavior can be attributed to the fact that at low temperatures the ability of the CaO to capture CO_2 is enhanced due to the exothermic nature of the carbonation reaction. Also, at high temperatures, greater amounts of steam will promote the steam reforming reaction, thus producing more CO_2 susceptible of being carbonated. Also in Figure 3 it can be seen that the mayor contamination of the product gas at intermediate temperatures (300-600°C) is due to methane formation where. Here in this plot the effect of the S/EtOH on the CH_4 composition is evident, since at temperatures below 700°C the methanation reactions above described are favored. However, as the amount of steam is increased the methane concentration at 500°C falls from 9% at S/EtOH = 3 to a value of 1.42% at S/EtOH = 6.5. This behavior can be explained by the enhancement of the steam reforming and WGS reactions at intermediate temperatures (300-600°C) by the use of a CO_2 absorbent, thus producing a higher H_2 content and lower methane concentrations.

Figure 4 shows the CO concentration (ppm) as a function of S/EtOH and temperature (left). Here in this plot the threshold value of 50 ppm is depicted by a dashed horizontal line to indicate the maximum amount of CO suitable as a feed in a PEMFC in order to avoid poisoning of the Pt catalyst.

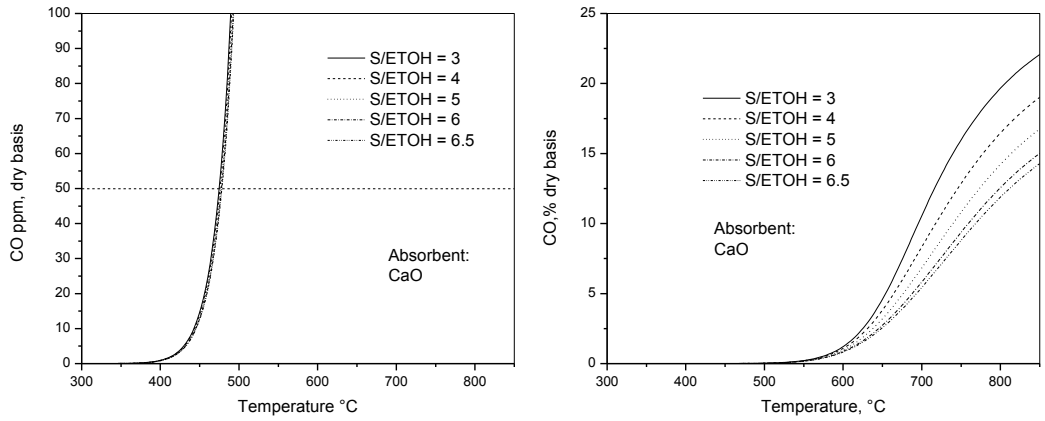

Figure 4. Equilibrium CO compositions for Ethanol Steam Reforming with CaO

It is important to notice that at temperatures below 500°C the effect of the S/EtOH is almost negligible, since there are no differences in CO composition at different steam contents in this region. A temperature of 478°C is necessary in order to assure a CO concentration equal or below 50 ppm CO. Also the effect of the CaO absorbent enhances the WGS and steam reforming reactions at temperatures lower than 550°C, thus avoiding a high CO content below this temperature. Higher temperatures than 550°C will increase the CO content in the product gas as the WGS would no longer be favored to react with steam.

*3.2.2 AER of Ethanol CaO*MgO Absorbent*

Figure 5 presents the hydrogen production ratio using calcined dolomite as a CO_2 absorbent in the steam reforming of ethanol system. Here it can be seen that there exist a locus of maximum hydrogen production as the S/EtOH increases. For example, at S/EtOH = 3 a HR of 4.74 is achieved at 725°C, while at S/EtOH = 6.5 a HR of 5.6 can be produced at 637°C. These results are for practical purposes the same as with the use of CaO as absorbent. However, the durability of this mineral is several orders of magnitude greater than CaO and this dolomite can withstand as many as 15 carbonation/decarbonation cycles without mayor deterioration [26].

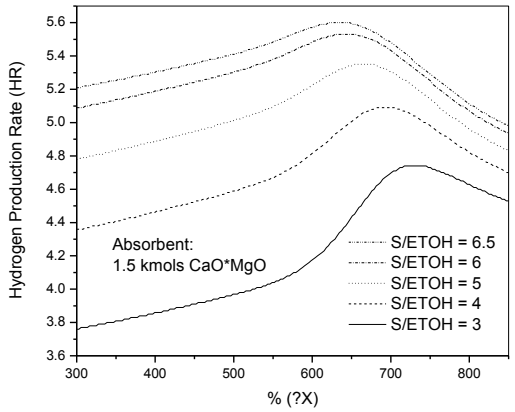

Figure 5. Equilibrium HR for Ethanol Steam Reforming with CaO*MgO

Figure 6 shows a three dimensional scheme, where the all the gaseous species concentrations (%) are plotted as a function of temperature and S/EtOH ratios.

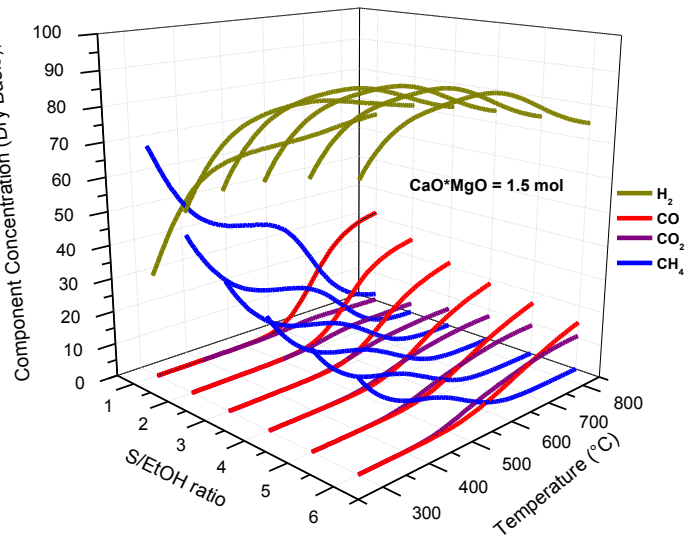

Figure 6. Equilibrium Compositions for Ethanol Steam Reforming with CaO*MgO

In this plot it can be seen how the general trends for each gaseous species behave as a function of temperature and S/EtOH ratio. For the case of hydrogen a concentration as high as 97% can be achieved at 510°C and S/EtOH = 6.5. At low temperatures the hydrogen concentration remains high, except for the cases of lower than stoichiometric S/EtOH values (< 3). For the cases of

carbon oxides (CO and CO_2) both concentrations are low at low temperatures as as consequence of the CO_2 absorption enhancement effect of the dolomite and gradually increase as temperature is raised (S/EtOH = 6) to values up to 15.3 and 11.5% for CO and CO_2, respectively. In Figure 6 it is evident that the mayor contaminant of the product gas is methane and this decreases as the temperature and S/EtOH ratio increases, thus enhancing the steam reforming reaction.

3.2.3 AER of Ethanol Na_2ZrO_3 Absorbent

Figure 7 presents the hydrogen production ratio (HR) as a function of temperature and S/EtOH ratio for the Na_2ZrO_3 absorbent. A maximum of HR of 5.49 can be obtained at 659°C and S/EtOH of 6.5. The shape of the curves resembles those observed for dolomite and CaO. However, the main difference is that at low temperatures (≈300°C) the H_2 product ratio remains lower than that observed for CaO or dolomite. This behavior can be explained in terms of the different thermodynamic nature of the absorbents. For example, the Gibbs free energy of their carbonation reactions for CaO, CaO*MgO and Na_2ZrO_3 at 300°C are -87.12, -79 and -65.87 kJ/mol, respectively. While at high temperatures (≈ 650°C) this difference in Gibbs free energy is small. Therefore, the ability for the Na_2ZrO_3 to capture CO_2 at low temperatures is hindered by the nature of the absorbent. However, at high temperatures the absorbent is able to generate a HR quite comparable to those above reported for CaO and dolomite (HR= 5.37 at 600°C and S/EtOH = 6).

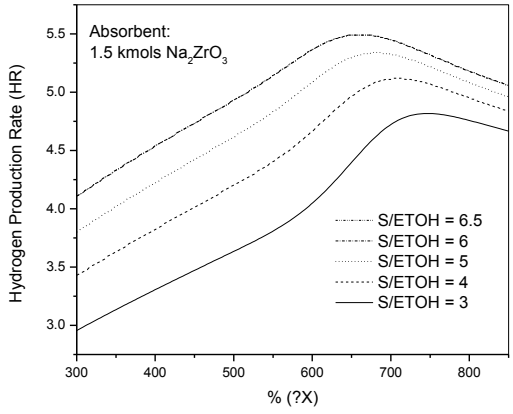

Figure 7. Equilibrium HR for Ethanol Steam Reforming with Na_2ZrO_3

Figure 8 presents the equilibrium concentrations of H_2, CO, CO_2 and CH_4 as a function of temperature and S/EtOH ratio for the Na_2ZrO_3 absorbent.

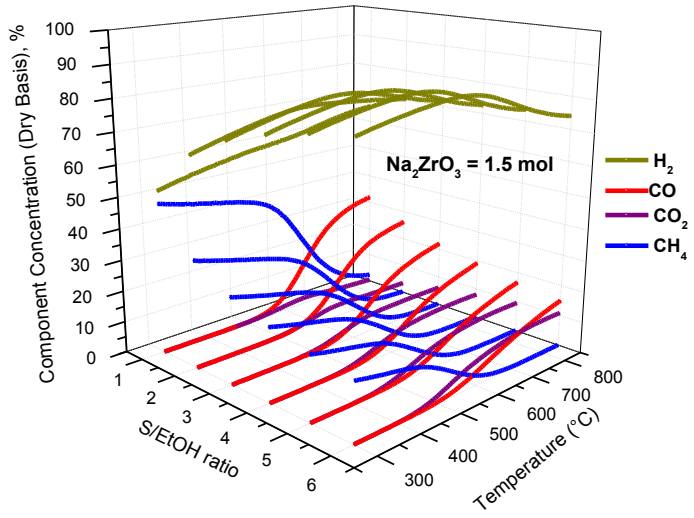

Figure 8. Equilibrium Compositions for Ethanol Steam Reforming with Na_2ZrO_3

In this plot it can be seen that even at low temperatures the hydrogen concentrations remain high (> 80% H_2) and eventually peak to a maximum of 96% H_2 at 512°C and S/EtOH = 6.5. Greater temperatures than 600°C will produce as in previous absorbents (CaO and CaO*MgO) a gradual decrease of the hydrogen content in the gas product. The production of carbon oxides at low temperatures are somewhat a bit higher than with previous absorbents because of the behavior above described. Finally, a temperature of 424°C is needed in order to assure a CO concentration of at ≤ 50 ppm.

3.2.4 AER of Ethanol Li_2ZrO_3 Absorbent

Results for the steam reforming of ethanol using Li_2ZrO_3 as CO_2 absorbent were very similar to those presented for Na_2ZrO_3. In fact, the shape of the HR as a function of temperature and S/EtOH was the same. Only slight differences appeared since a maximum HR of 5.5 can be obtained at 651°C and S/EtOH of 6.5. Otherwise, the trends and shapes of all gaseous species in

the product gas were essentially the same, with a maximum H_2 concentration of 95.5% at 504°C and S/EtOH of 6.5. All these similarities can be explained in terms of the thermodynamic nature of these absorbents. A comparison in terms of the Gibbs free energy of the carbonation reactions (10) and (11) at 600°C results in very small differences since Na_2ZrO_3 and Li_2ZrO_3 show values of -24.58 and -23.53 kJ/mol, respectively.

3.2.5 AER of Ethanol Li_4SiO_4 Absorbent

Figure 9 shows the hydrogen production ratio (HR) as a function of temperature and S/EtOH ratio for the Li_4SiO_4 absorbent. Hre it can be observed that a maximum of HR of 5.37 can be obtained at 656°C and S/EtOH of 6.5.

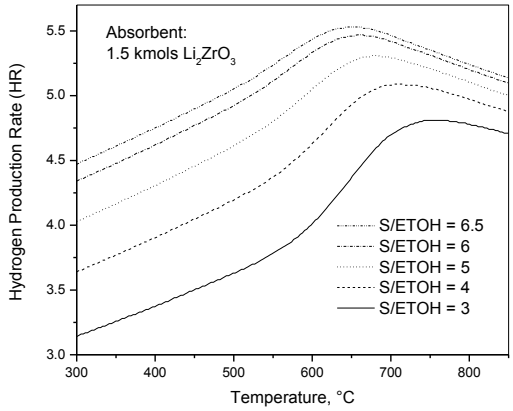

Figure 9. Equilibrium HR for Ethanol Steam Reforming with Li_4SiO_4

The shape of the HR curves appeared to be closer to each other at each S/EtOH ratio compared to the ones for Na_2ZrO_3 and Li_2ZrO_3. This behavior reflects the fact that the hydrogen production is somewhat limited by the absorption ability of Li_4SiO_4 to capture CO_2, especially at low temperatures (≈ 300°C). This is more evident when a comparison is made between the curves for S/EtOH ratios 6 and 6.5. This means that the maximum hydrogen production ratio (HR) can be found at ratios closer to 6 rather than with Na_2ZrO_3 and Li_2ZrO_3, which maximum appears to be closer to 6.5.

Figure 10 shows the equilibrium concentrations of H_2, CO, CO_2 and CH_4 as a function of temperature and S/EtOH ratio for the Li_4SiO_4 absorbent.

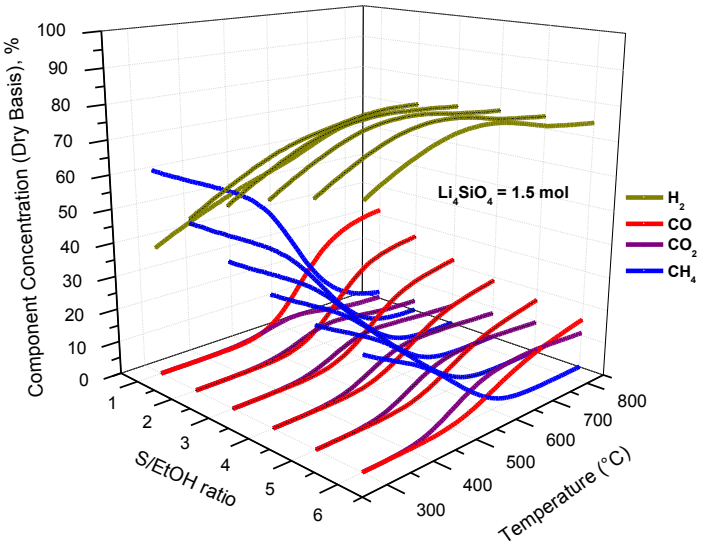

Figure 10. Equilibrium Compositions for Ethanol Steam Reforming with Li_4SiO_4

According to results from Figure 10 it can be seen that the trends and shapes of all gaseous species in the product gas were similar to those presented for the zirconates. However, the values for hydrogen concentrations were lower accompanied with higher values of methane, especially at low temperatures. This was reflected in the maximum H_2 concentration which was 85.3% at 600°C and S/EtOH of 6.

3.2.6 Absorbent Comparison for Ethanol Reforming

Table 1 presents a summary of simulation results for the steam reforming of ethanol with and without the use of a CO_2 absorbent. Conditions reported in this table were close to the maximum hydrogen production obtained for each absorbent and these were; S/EtOH = 6:1 and at 600°C. This temperature was chosen because it represents the average of the maximum hydrogen production in all performed calculations. This Table shows the evident limitation of the steam reforming of ethanol (SR) without absorbent, since only 4.6 mols of H_2 were produced per mol of ethanol. Even at this relatively high temperature the amounts of CO, CH_4 and CO_2 are relatively

high, with 0.23, 0.54 and 1.23 mols at equilibrium, respectively. Also the hydrogen concentration was only of 69%. The expected enhancement with the use of a CO_2 absorbent is clear when a comparison is made with respect to the values obtained for CaO. In Table 1 the increase in hydrogen production was of 19.2% greater with the use of CaO. Consequently, the other gaseous species were reduced. CO produced was reduced 3.3 times, while CO_2 was reduced 15.4 times. Also, methane was reduced 10.8 times. All this is translated in a very high hydrogen concentration which for this absorbent reached 97%.

Table 1. Summary of Simulation Results for Ethanol Steam Reforming at 600°C

Absorbent	Mols at Equilibrium				Parameters	
	H_2	CO	CO_2	CH_4	S/EtOH ratio	$\%H_2$
CaO	5.7	0.07	0.08	0.05	6:1	97
CaO*MgO	5.5	0.11	0.14	0.09	6:1	94
Na_2ZrO_3	5.4	0.13	0.20	0.12	6:1	92
Li_2ZrO_3	5.3	0.13	0.22	0.13	6:1	92
Li_4SiO_4	5.0	0.18	0.45	0.24	6:1	85
No Absorbent	4.6	0.23	1.23	0.54	6:1	69

Other absorbents behaved similarly to the results presented in the previous section. For example, calcined dolomite (CaO*MgO) exhibited only a small difference in results with respect to CaO. Since, the hydrogen production was reduced only 3.5%, while CO and CO_2 were increased 57 and 75% from the values produced using CaO. However, these values were 16% higher in H_2 production and 25% in hydrogen concentration (94%) compared with conventional SR (69%). Results for the zirconate absorbents Na_2ZrO_3 and Li_2ZrO_3 were very similar between them and to the ones for CaO*MgO as can be seen in Table 1. For example, hydrogen production for Na_2ZrO_3 and Li_2ZrO_3 were 5.4 mols and 5.3 at equilibrium, respectively compared to 5.5 for CaO*MgO. Equilibrium mols of CO followed the same trend, while CO_2 mols presented only a slight decrease of the zirconate absorbents compared to those produced by calcined dolomite (0.14 compared to 0.20 and 0.22) and the same trend occurred with methane formation. However, hydrogen concentration was just slightly less for the zirconates (92%) compared to the concentration produced by calcined dolomite (94%).

Finally, Li_4SiO_4 was the absorbent that produced the lowest hydrogen production and higher by product concentrations (CO, CO_2 and CH_4). This was translated in a lower hydrogen concentration of only 85%. This behavior can be attributed to the thermodynamic nature of this absorbent. For example, if the Gibbs free energy of carbonation at 600°C is compared between the zirconates and the lithium orthosilicate, there exists a significant difference with values of -24.6 and -23.5 kJ/mol for Na_2ZrO_3 and Li_2ZrO_3, respectively to a value of -12.5 kJ/mol for Li_4SiO_4.

Therefore, a crucial feature within the hydrogen production through the absorption enhanced reforming (AER) of ethanol and/or methanol resides in nature of the CO_2 solid absorbent, which apart from favorable thermodynamics, must present adequate absorption capacity and fast absorption-regeneration kinetics. Several researches have focused their studies in the effects of pressure, temperature and gas reactant composition on absorbents based on calcium oxide (CaO) using the thermogravimetric (TGA) experimental technique [27, 28]. However, sintering of these materials reduce their performance after several absorption-regeneration cycles. Calcined dolomite (CaO*MgO) have shown to better perform in CO_2 absorption at high temperatures compared to CaO in multicycle tests [28]. Unfortunately, this mineral origin absorbent requires high regeneration temperatures ($T \geq 950$ °C) that produce degradation of the material after 10 absorption-regeneration cycles. Bandi et al. [29] proposed the use of the mineral huntite ($Mg_3Ca(CO_3)_4$) exhibiting good regeneration performance. However, this absorbent has several disadvantages such as: a high regeneration temperature and low CO_2 capacity. Also of mineral origin the $Mg_6Al_2(CO_3)(OH)_{16}*4H_2O$ hydrotalcite was proposed by Hufton et al. [30] and Ding and Alpay [31] which used this CO_2 adsorbent at moderate temperatures (400-500 °C) resulting in low adsorption capacity.

Studies from López Ortiz et al., [12] have shown the superior performance of Na_2ZrO_3 as an alternate synthetic CO_2 solid absorbent compared to expensive lithium-base absorbents (Li_2ZrO_3

and Li_4SiO_4) (Nakagawa and Ohashi [32] and Kato et al, [33]). This behavior was attributed on its excellent thermal stability, kinetics and CO_2 capture capacity features.

Recently, Ochoa Fernandez et al., [34] have experimentally evaluated several synthetic CO_2 absorbents, under the AER of methane reaction scheme, such as: Li_2ZrO_3, $LiSiO_4$ and Na_2ZrO_3 and concluded that Na_2ZrO_3 is the one that better performed towards high methane conversions, hydrogen purity and reaction kinetics. Furthermore, Jakobsen and Halmøy [35] performed a reactor modeling of the sorption enhanced steam methane reforming using CaO, Li_4SiO_4 and Na_2ZrO_3 and also concluded that Na_2ZrO_3 is the most efficient absorbent with the highest hydrogen production ratio (92.6%) compared to CaO (79.3%) and Li_4SiO_4 (82.1%) at the same reaction conditions in a temperature range from 600°C to 800°C.

Therefore, from the above presented thermodynamic analysis of the absorption enhanced ethanol reforming it can be concluded that Na_2ZrO_3 is a promising alternate absorbent with comparable thermodynamics and greater kinetics and stability. Modeling results agreed with experimental evaluation of ethanol reforming using CaO*MgO, and Na_2ZrO_3.

3.3 Methanol Steam Reforming System

3.3.1 Gas Product Distribution without Absorbent

Figure 11 shows the equilibrium hydrogen production ratio (HR) and H_2 concentration (%) as a function of temperature (350-800°C) and S/MeOH ratio (1-6). In this Figure it can be seen that a maximum of 2.22 HR was reached at 725°C and S/MeOH of 1 (stoichiometric condition) As the S/MeOH is increased from 1 to 6 the HR also raised towards values located at lower temperatures. For example, a maximum of 2.76 HR was achieved at 595°C and S/MeOH of 6.

This behavior, as in the case of the ethanol reforming, can be explained by the promotion of the methanation reactions at low temperatures (300-500°C). On the other hand, at stoichiometric conditions (S/MeOH = 1), a maximum hydrogen concentration of 69% was reached at 731°C.

Again, the increase in S/MeOH ratio resulted in higher hydrogen concentrations at lower temperatures. Since a value of 73% was reached at 576°C and a S/MeOH of 6.

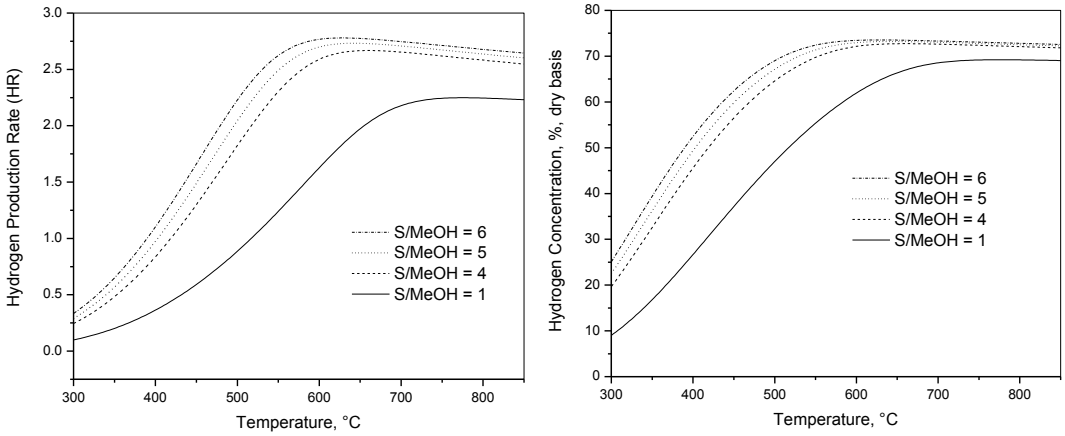

Figure 11. Equilibrium HR and H_2 for Methanol Steam Reforming

Figure 12 depicts the carbon oxide equilibrium compositions for methanol reforming. In this Figure it can be seen that CO is produced at relatively small concentrations at low temperatures (300-500°C) and as temperature increases CO concentrations also is raised and can be as high as 19.6% at 700°C and S/MeOH ratio of 6. CO production at high temperature is generated through the dry reforming and steam reforming reactions, reverse reactions (17) and (20), respectively. That is the reason why the CO concentration is increased at high temperatures (T > 500°C), while CO_2 and CH_4 concentrations are lowered in this particular region. Also, in this Figure it can be seen that a low level of 50 ppm of CO never is reached within the generated data, since the lowest possible CO concentration is 0.032% which represents a value of 327 ppm of CO at 300°C and S/MeOH ratio of 6:1. Also in this Figure the CO_2 concentration is high at relatively low temperatures (300-500°C). This is due to the methanation reaction (17), which favors the production of CO_2 and methane at low temperatures. Also, as temperature is increased CO_2 is reduced due to the dry reforming reaction (reverse reaction 17) and to the fact that the WGS is no longer favorable at these conditions.

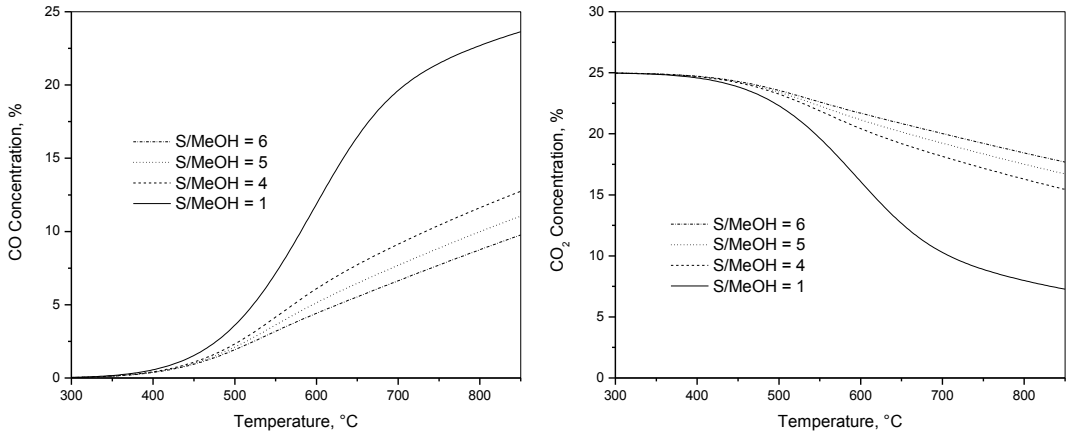

Figure 12. Equilibrium CO and CO_2 Concentrations for Methanol Steam Reforming

Figure 13 presents the methane concentration profile as a function of temperature and S/MeOH ratio. In this plot it can be seen, as pointed out above, that methane concentrations at low temperatures are high due to the promotion of the methanation reactions (17-21). Also, as temperature increased these concentrations are reduced due to the promotion of the steam and dry methane reforming reactions.

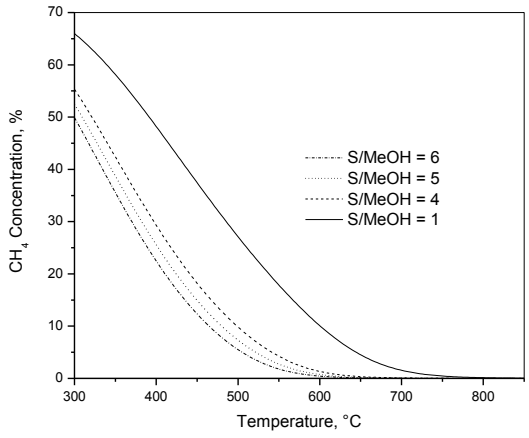

Figure 13. Equilibrium CH_4 Concentration for Methanol Steam Reforming

Also, in this Figure it can be seen that as the S/MeOH ratio is increased the methane concentration is reduced; particularly at high temperatures (T > 500°C).This behavior is

consistent with the fact that a higher steam concentration will favor the steam methane reforming reaction towards a higher production of H_2 and CO_2.

3.3.2 Gas Product Distribution with CaO as CO_2 Absorbent

Figure 14 shows a three dimensional scheme, where the all the gaseous species concentrations (%) are plotted as a function of temperature and S/MeOH ratios for the steam reforming of methanol with CaO as a CO_2 absorbent.

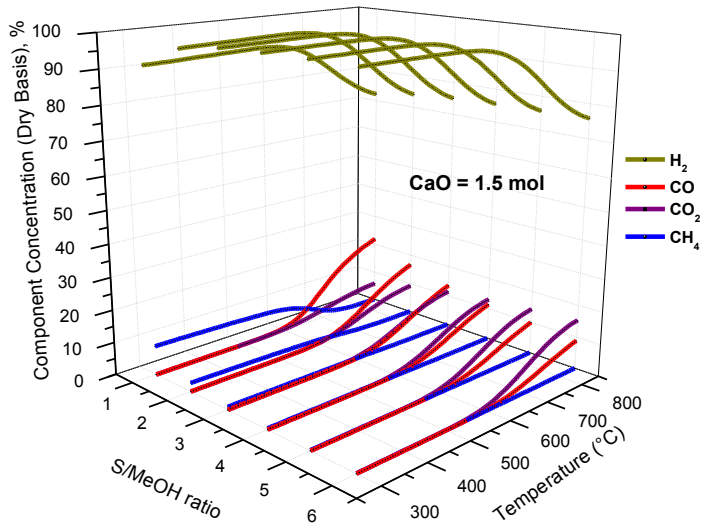

Figure 14. Equilibrium Compositions for Methanol Steam Reforming with CaO

In this plot it can be seen how the general trends for each gaseous species behave as a function of temperature and S/MeOH ratio. For the case of hydrogen a concentration as high as 99.9% can be achieved at 450°C and S/MeOH = 6. At low temperatures the hydrogen concentration remains high, even for the case of the stoichiometric value (92% H_2 at 544°C, S/MeOH = 1). For carbon oxides (CO and CO_2) both concentrations are very low at low temperatures as a result of the CO_2 absorption enhancement effect of CaO and gradually increased as temperature was raised (T > 500°C) to values up to 8.9 and 15.3% for CO and CO_2 (S/MeOH = 6), respectively. Furthermore, a temperature of 485°C is needed in order to assure a CO concentration of ≤ 50 ppm.

In Figure 14 it is clear that the only significant contaminant of the product gas at low temperatures is methane and this decreased as the temperature and S/MeOH ratio also increased, thus enhancing the steam reforming reaction. Greater values of S/MeOH = 2 will insure very low CH_4 concentrations (less than 1%) in all the temperature range studied (300-850°C).

*3.3.3 Gas Product Distribution with CaO*MgO as CO_2 Absorbent*

Figure 15 shows the equilibrium concentrations of H_2, CO, CO_2 and CH_4 as a function of temperature and S/MeOH ratio for the CaO*MgO absorbent.

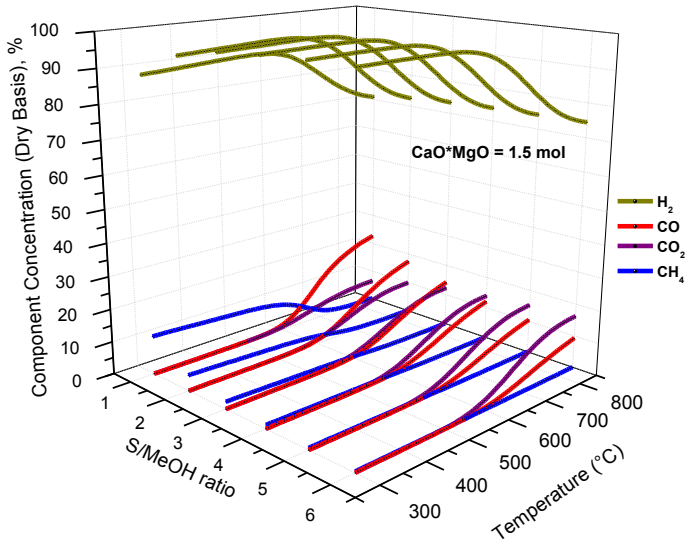

Figure 15. Equilibrium Compositions for Methanol Steam Reforming with CaO*MgO

In this plot it can be seen that the concentration profiles of each species generated with the CaO*MgO absorbent are for practical purposes the same as for CaO. The only apparent difference is the slightly higher levels of methane formation at low temperatures (300-500°C) and in the range of S/MeOH ratios from 1 to 3. Also, a temperature of 464°C is needed in order to assure a CO concentration of ≤ 50 ppm.

3.3.4 Gas Product Distribution with Na_2ZrO_3 as CO_2 Absorbent

Figure 16 shows results of the steam reforming of methanol using Na_2ZrO_3 as a CO_2 absorbent. In this Figure equilibrium concentrations for gaseous species H_2, CO, CO_2 and CH_4 are plotted as a function of temperature and S/MeOH ratio.

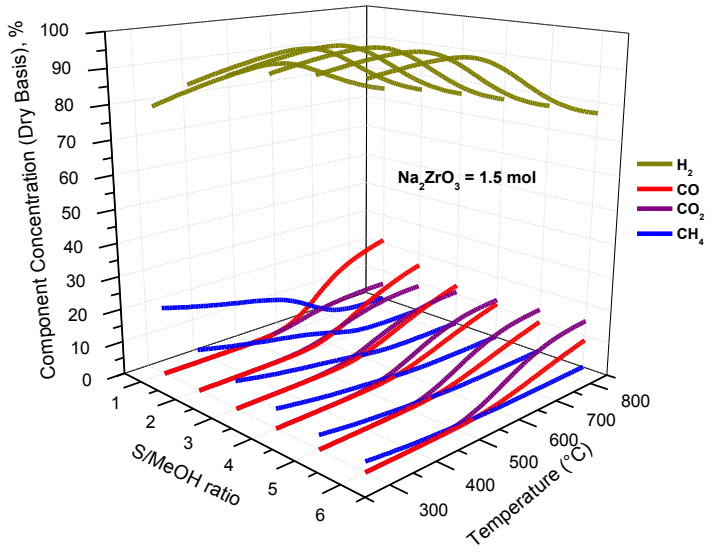

Figure 16. Equilibrium Compositions for Methanol Steam Reforming with Na_2ZrO_3

In this plot it can be seen that even at low temperatures the hydrogen concentrations remain high (> 80% H_2) and eventually peak to a maximum of 98.7% H_2 at 472°C and S/MeOH = 6. Greater temperatures than 600°C will produce as in previous absorbents (CaO and CaO*MgO) a gradual decrease of the hydrogen content in the product gas. A higher production of carbon oxides than with the use of calcium absorbents is observed at high temperatures with values as high as 4 and 11.2% for CO and CO_2, respectively (T= 700°C and S/MeOH= 6). This behavior can be explained by thermodynamic nature of the CaO absorbent, which absorption Gibbs free energy at 600°C is 1.69 times more negative than for the Na-based absorbent (Na_2ZrO_3). Finally, a temperature of 427°C is needed in order to assure a CO concentration of ≤ 50 ppm.

3.3.5 Gas Product Distribution with Li_2ZrO_3 as CO_2 Absorbent

Figure 17 presents a three dimensional plot where results of the steam reforming of methanol equilibrium concentrations using Li_2ZrO_3 as a CO_2 absorbent are presented as a function of temperature and S/MeOH ratio.

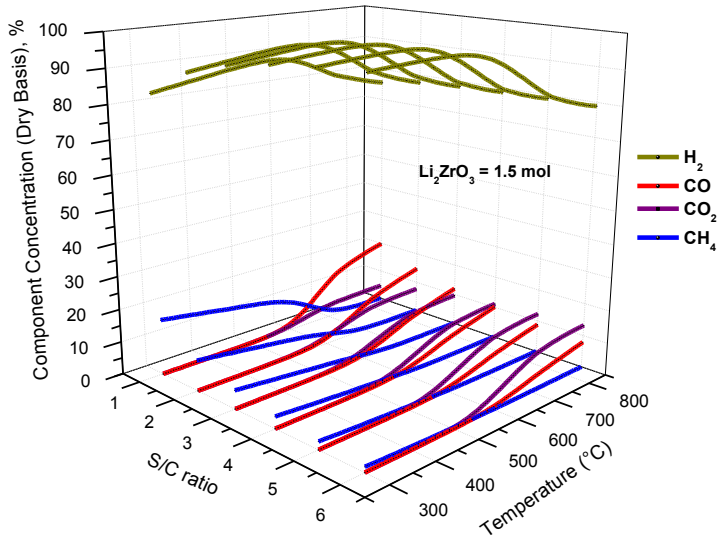

Figure 17. Equilibrium Compositions for Methanol Steam Reforming with Li_2ZrO_3

Results from Figure 17 using Li_2ZrO_3 make evident that the trends and equilibrium concentrations are almost the same as with Na_2ZrO_3. However, there is a slight difference mainly in the methane formation at low temperatures, which for the Na-based absorbent is slightly higher than for Li_2ZrO_3. For example a value of 16.8% CH_4 was generated at 300°C and S/MeOH ratio of 1 (stoichiometric condition), while a value of 20.4 was generated by Na_2ZrO_3. Other than that results were essentially the same between zirconate absorbents. Finally, a temperature of 439°C is needed in order to insure a CO concentration of ≤ 50 ppm with this absorbent.

3.3.6 Gas Product Distribution with Li_4SiO_4 as CO_2 Absorbent

Figure 18 shows the equilibrium concentrations of H_2, CO, CO_2 and CH_4 as a function of temperature and S/MeOH ratio for the Li_4SiO_4 absorbent.

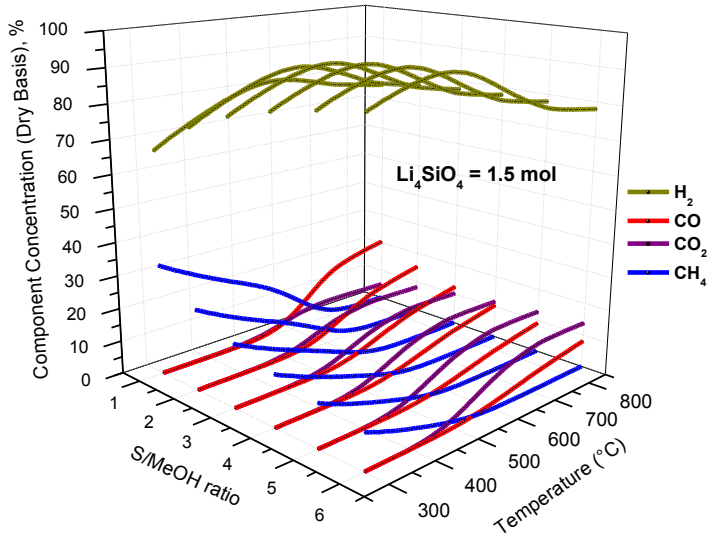

Figure 18. Equilibrium Compositions for Methanol Steam Reforming with Li_4SiO_4

Results from Figure 18 indicate that the trends and shapes of all gaseous species in the product gas were similar to those presented for the zirconates. However, the values for hydrogen concentrations were lower and accompanied with higher values of methane, especially at low temperatures. This was reflected in the maximum H_2 concentration which was 88.3% at 600°C and S/EtOH of 6. Also, a temperature of 391 °C is needed in order to insure a CO concentration of ≤ 50 ppm with this absorbent.

3.3.7 Absorbent Comparison for Methanol Reforming

Table 2 shows a summary of simulation results for the steam reforming of methanol with and without the use of a CO_2 absorbent. Conditions reported in this table were close to the maximum hydrogen production obtained for each absorbent and these were; S/MeOH = 6:1 and at 600°C. This temperature was chosen because it represents the average of the maximum hydrogen production in all performed calculations. This Table exhibits the evident limitation of the steam reforming of methanol (SR) without absorbent, since only 2.77 mols of H_2 were produced per mol of methanol. Even at this relatively high temperature the amounts of CO, CO_2 and CH_4, are relatively high with 0.166, 0.816 and 0.017 mols at equilibrium, respectively. Also the hydrogen

concentration was only of 73%. The expected enhancement with the use of a CaO absorbent was not very significant, since a comparison between this with respect to SR without the use of an absorbent only represents an increase of 7% in hydrogen production. However, the main difference is achieved in the byproduct gaseous concentrations, which all were significantly reduced. Using CaO, CO produced was reduced 16.6 times, while CO_2 was reduced 18.5 times. Also, methane was reduced 8.5 times. All this was translated in a very high hydrogen concentration, which for this absorbent was 98%, an increase of about 25% with respect to SR without absorbent.

Table 2. Summary of Simulation Results for Methanol Steam Reforming at 600°C

Absorbent	Mols at Equilibrium				Parameters	
	H_2	CO	CO_2	CH_4	SMetOH ratio	$\%H_2$
CaO	2.98	0.010	0.044	0.002	6:1	98
CaO*MgO	2.97	0.020	0.088	0.003	6:1	96
Na_2ZrO_3	2.91	0.038	0.169	0.006	6:1	98
Li_2ZrO_3	2.95	0.031	0.138	0.005	6:1	94
Li_4SiO_4	2.90	0.067	0.306	0.009	6:1	88
No Absorbent	2.77	0.166	0.816	0.017	6:1	73

Other absorbents behaved similarly to the results presented in the previous section. For example, calcined dolomite (CaO*MgO) exhibited only a small difference in results with respect to CaO. Since, the hydrogen production was practically the same (2.98 and 2.97), while CO and CO_2 were doubled from the values produced using CaO. However, these values were only 2% higher in H_2 concentration (96%) compared with CaO and 23% higher to conventional SR (73%). Results for the zirconate absorbents Na_2ZrO_3 and Li_2ZrO_3 were very similar between them and to the ones for CaO*MO as can be seen in Table 2. For example, hydrogen production for Na_2ZrO_3 and Li_2ZrO_3 were 2.91 and 2.95 mols at equilibrium, respectively compared to 2.97 for CaO*MgO. Equilibrium mols of CO followed the same trend, while CO_2 mols presented only a slight increase of the zirconate absorbents compared to those produced by calcined dolomite (0.088 compared to 0.169 and 0.138) and the same trend occurred with methane formation. However,

hydrogen concentration was just slightly lower for the Na_2ZrO_3 (98%) compared to the concentration produced by calcined dolomite (96%) and Li_2ZrO_3 (94%).

Similarly to the case of ethanol reforming, methanol reforming using Li_4SiO_4 produced the lowest hydrogen production and higher byproduct concentrations (CO, CO_2 and CH_4). This was translated in a lower hydrogen concentration of only 88%. This behavior can be attributed to the limited thermodynamic nature of this absorbent as pointed out before in the ethanol reforming section.

Hence, from the above thermodynamic analysis for the absorption enhanced methanol reforming it can be concluded that Na_2ZrO_3 and Li_2ZrO_3 are both promising alternate absorbents with comparable thermodynamics to CaO based absorbent. However, greater kinetics and stability can be achieved with the use of Na_2ZrO_3 [12]. Recent experimental results dealing with conventional methanol steam reforming have used Cu-based catalyst [36, 37] and therefore, there is the chance to suppress CH_4 over this catalyst. However, it is well known that Cu-based catalysts suffer from deactivation due sintering of the active Cu at the high operating temperatures (450-600°C) of the AER process. Therefore, other materials such as Ni-based catalysts can be used in the AER of methanol, as reported by Lysikov et al. [38].

3.4 Carbon Formation

3.4.1 Carbon Formation for the Ethanol Reforming System

Figure 19 shows the effect of steam to ethanol molar ratios and temperature on the number of moles of carbon (graphite) produced in the steam reforming of ethanol (SR) and through AER using all the absorbents studied in the present work. In this plot the maximum amount of carbon produced is plotted as a function of the S/EtOH ratio from 0 to 1. In each data point the temperature where the maximum carbon formation was found is specified. Also, in this plot there is a table where the minimum temperature reached without carbon formation is depicted as a function of the type of CO_2 absorbent. The temperature in this table can be defined as the

minimum temperature, necessary to inhibit carbon deposition at the minimum S/EtOH ratio for each absorbent.

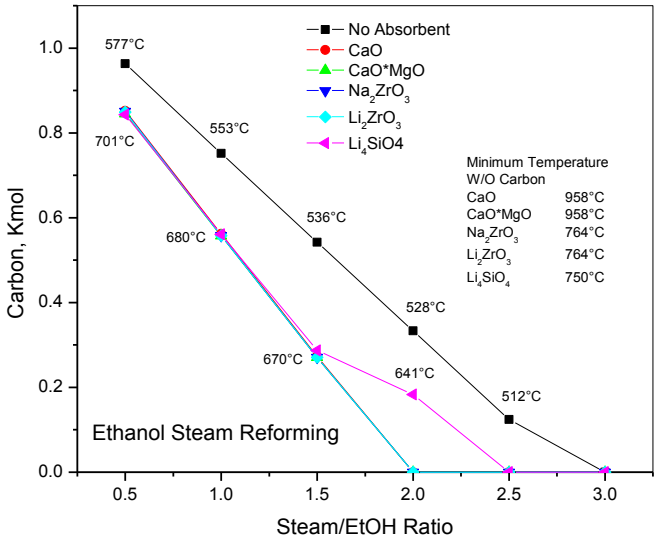

Figure 19. Equilibrium Maximum Carbon Formation for Ethanol Steam Reforming with Absorbents

In this plot is evident that without the use of a CO_2 absorbent carbon formation is favored and its maximum is reached at lower temperatures than with the use of an absorbent. The SR produced a maximum carbon formation of 0.96 kmol per mol of ethanol fed to the system at S/EtOH ratio of 0.5 and it is found at a temperature of 577°C. Greater temperatures and S/EtOH ratios will produce lower amounts of carbon and a S/EtOH ratio greater than 2.5 and temperatures higher than 512°C will insure a carbon free operation under this system. Surprisingly, the use of different CO_2 absorbents produced maximum carbon formations at the same temperatures and S/EtOH ratios, with only the exception of Li_4SiO_4 that deviated from this behavior at greater S/EtOH ratio than 1.5 and at temperatures lower than 670°C. Therefore, from this point it can be seen that Li_4SiO_4 is more prompted to produce greater amounts of carbon than the other absorbents studied. Furthermore, for the other absorbents, greater S/EtOH ratios than 1.5 will produce lower amounts of carbon. Carbon free operation can be found at S/EtOH ratios greater than 2.0 and at temperatures higher than 958°C for CaO based absorbents (CaO and CaO*MgO) and higher than 760°C for the synthetic absorbents. It is important to mention that synthetic

absorbents (Na_2ZrO_3, Li_2ZrO_3 and Li_4SiO_4) have the tendency to present lower carbon free operating temperatures than with the use of CaO-based absorbents. The behavior related to the lower carbon formation found with the use of a CO_2 absorbent (very low risk of carbon formation), is directly related to the reduction in CO content. Li [39] confirmed in his thermodynamic study, that graphite formation is suppressed with CO_2 absorption. According to this author, the Boudouard reaction:

$$2CO(g) = CO_2(g) + C(s) \qquad \Delta H°_{298} = -172.5 \text{ kJ/mol} \qquad (22)$$

is shifted towards the reverse Boudouard reaction because its equilibrium constant is related to the square of CO concentration.

3.4.2 Carbon Formation for the Methanol Reforming System

Figure 20 shows the effect of S/MeOH ratios and temperature on the number of moles of carbon generated under the steam reforming of methanol and through the AER systems. Again as in Figure 16, in this scheme the maximum amount of carbon produced is plotted as a function of the S/EtOH ratio from 0 to 1. In each data point the temperature where the maximum carbon formation was found is specified. Also, in this plot there is a table where the minimum temperature reached without carbon formation is depicted as a function of the type of CO_2 absorbent. The temperature in this table can be defined as the minimum temperature, necessary to inhibit carbon deposition at the minimum S/MeOH ratio for each absorbent. As in the case of ethanol reforming it is clear that the use of a CO_2 absorbent produce a low tendency to deposit carbon. Without the use of an absorbent, the maximum production of carbon (0.29 mol/mol of methanol) occurs at 536°C at a S/MeOH ratio of 0.2:1. Similar temperatures and larger S/EtOH ratios will produce lower amounts of carbon. In order to insure carbon free operation under this system steam to methanol ratios greater than 0.8 and temperatures higher than 520°C are needed.

Similarly to the ethanol system, the use of different CO_2 absorbents generated equal maximum carbon formations for all the absorbents at the same temperatures (300-850°C) and S/EtOH ratios studied (0.2-1). Therefore, the carbon free operation region is the one that presents greater S/EtOH ratios than 0.6 and temperatures higher than 778°C under AER of methanol reaction.

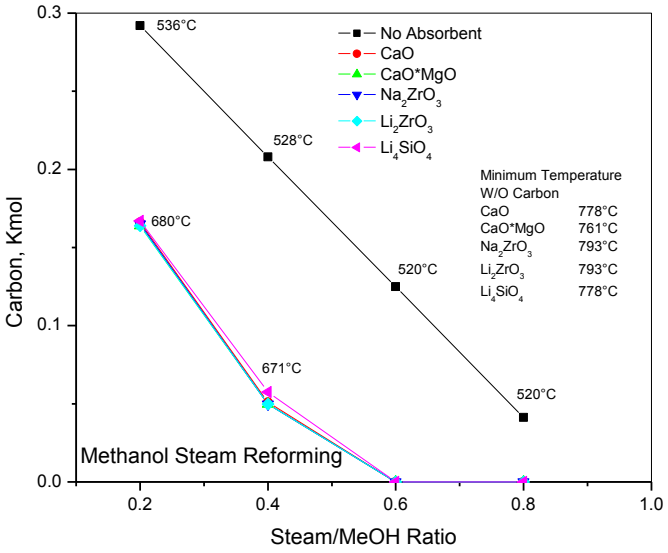

Figure 20. Equilibrium Maximum Carbon Formation for Methanol Steam Reforming with Absorbents

Alos, in Figure 20 it can be observed that either CaO-based (CaO and CaO*MgO) and synthetic absorbents (Na_2ZrO_3, Li_2ZrO_3 and Li_4SiO_4) have the tendency to present relatively the same carbon free operating temperatures. These varied from 778°C (CaO and Li_4SiO_4) to 793°C (Li_2ZrO_3 and Na_2ZrO_3). Some of these results (without absorbent) are in agreement with the data reported by Faungnawakij et al. [40].

3.5 Thermal Efficiency Analysis

3.5.1 Thermal Efficiency for Ethanol Reforming and with CO_2 Absorbents

Table 3 shows the influence of the S/EtOH ratio on the thermal efficiency (η) at 600°C. In this Table the temperature of 600°C was chosen because at this condition most of the systems achieved their maximum hydrogen production and concentrations (see previous sections). For the case where no absorbent was employed, the thermal efficiency of the process increases as the

S/EtOH ratio also increases. However, as suggested by He et al. [18] the cost of the energy for generating extra steam can be compensated by promoting hydrogen production in the reforming process. For example at S/EtOH ratio of 5 the thermal efficiency is 64%, while an increase to 6 and produced an efficiency of 66.3%, which reflects the behavior above described. However, a further increase in S/EtOH ratio to 6.5 only produced a marginal increase to 67% in thermal efficiency. These values are in agreement with studies reported by Lima da Silva and Müller [8]. This above behavior was expected, since the one of the factors that has a great impact in the thermal efficiency is the amount of hydrogen produced and a careful examination of Figure 1 reveals that also in that plot an increase in S/EtOH ratio from 5 to 6 and even to 6.5 produced only a marginal increase in hydrogen production. Therefore, here it can be concluded that S/EtOH = 6 and 600°C are a good choice of conditions where all the absorbents can be compared in terms of thermal efficiency.

Table 3. Summary of Thermal Efficiency Results for Ethanol Steam Reforming at 600°C.

Absorbent	S/EtOH Molar Ratio	Thermal Efficiency (η, %)
No Absorbent	5	64.0
	6	66.3
	6.5	67.0
CaO	6	82.6
	6.5	81.9
CaO*MgO	6	80.0
Na_2ZrO_3	6	78.3
Li_2ZrO_3	6	77.9
Li_4SiO_4	6	73.5

Also in Table 3 the values for the thermal efficiency for the AER of ethanol are reported for every absorbent studied. The use of CaO produced a thermal efficiency of 82.6%, while an increase in S/EtOH ratio of 6.5 slightly reduced its efficiency to a value of 81.9%. This means

that the amount of steam generated can eventually reduce the efficiency of the system, since not only the gaseous species absorb the heat provided by the steam but the solid absorbent also takes some of that heat. However, the advantage in the use of a CO_2 absorbent (CaO) resulted in an increase in thermal efficiency of 16.3%, which represents significant energy savings generated by the AER process scheme. The use of calcined dolomite only reduced the thermal efficiency in 2% with respect to CaO. This is understandable if it is considered that an inert (MgO) is used along with the main absorbent compound (CaO). The same behavior is observed for Na_2ZrO_3, Li_2ZrO_3 and Li_4SiO_4, which were resulted in slightly lower efficiencies than CaO with values of 78.3, 77.9 and 73.5, respectively. The differences observed can be explained in terms of their differences in regeneration temperatures, heats of reaction and regeneration and hydrogen produced. Therefore, it is a complex combination of parameters that generates a specific thermal efficiency. From the results of Table 3 it can be seen that the synthetic absorbent that better performs in terms of thermal efficiency is Na_2ZrO_3, followed by Li_2ZrO_3 with a small difference, while Li_4SiO_4 presented a limited thermal efficiency.

3.5.2 Thermal Efficiency for Methanol Reforming and with CO_2 Absorbents

Table 4 presents results from calculations of the thermal efficiency (η) at 600°C at different S/EtOH ratios. Again, here in this Table a temperature of 600°C was chosen because at this condition most of the systems achieved their maximum hydrogen production and concentrations (see previous sections). Without the use of absorbent the thermal efficiency increased as the S/MeOH ratio also increased from 54% at S/MeOH of 1 (stoichiometric condition) to 67.5% at S/MeOH of 4. A further increase in S/MeOH ratio resulted in a decrease in thermal efficiency to values of 65.5 and 62.9% for S/MeOH ratios of 5 and 6, respectively. These results are in agreement with reported data by He et al. [25] and Lima da Silva and Müller [8]. Therefore an optimal S/MeOH ratio of 4 was employed for comparing the effect of each absorbent on the thermal efficiency.

Table 4 reports the values for the thermal efficiency of the AER of methanol for every CO_2 absorbent studied. The use of CaO produced a thermal efficiency of 77.3% at a S/EtOH ratio of 4, while an increase in S/EtOH ratio to0 5 and 6 reduced significantly its efficiency to values of 72.3 and 67.8%. This means that the amount of steam generated can eventually hurt the efficiency of the system, a lot heat is needed in order provide high S/MeOH ratios greater than 4. Additionally, not only the gaseous species absorb the heat provided by the steam but the solid absorbent also takes some of that heat. Nevertheless, the advantage in the use of a CO_2 absorbent (CaO) resulted in an increase in thermal efficiency of 9.8%, which represents energy savings generated by the AER process scheme.

Table 4. Summary of Thermal Efficiency Results for Methanol Steam Reforming at 600°C.

Absorbent	S/MetOH Molar Ratio	Thermal Efficiency (η, %)
No Absorbent	6	62.9
	5	65.5
	4	67.5
	1	54.5
CaO	6	67.8
	5	72.3
	4	77.3
CaO*MgO	4	76.3
Na_2ZrO_3	4	75.6
Li_2ZrO_3	4	75.4
Li_4SiO_4	4	72.9

The use of calcined dolomite reduced the thermal efficiency 1% with respect to CaO. Therefore, the impact of introducing an inert such as MgO only produced a minor effect over the thermal efficiency. Whereas, the use of the zirconates, Na_2ZrO_3 and Li_2ZrO_3, resulted in almost identical values for this system (75.6 and 75.4%, respectively) and only represented a reduction of about 1.7% with respect to CaO. These absorbent systems are promising since their differences with

respect to CaO are minor and they present the advantages of being materials with high thermal stability and durability. Finally, from results of Table 4 it can be seen that Li_4SiO_4 presented a limited thermal efficiency of 72.9%, which agrees well with its performance during the hydrogen production thermodynamic analysis evaluation.

Additionally, for both biofuels analyzed (ethanol and methanol), it should be observed that in the AER process the highest efficiencies occur in a limited range of steam-to-fuel ratios (6 for ethanol and 4 for methanol).

3.6 Optimal Operating Conditions for AER process

For both bio-fuels, under the AER system, it can be seen that it is possible to obtain a hydrogen concentration of ≈ 99% purity at 1 atm, 500°C and S/MeOH = 4 and 600°C and S/EtOH = 6. However, in order to achieve a CO concentration below 50 ppm intended for PEMFC applications a temperature around 450°C is needed, which represents a decrease in hydrogen production as well as in hydrogen purity from the above described conditions. Therefore, a preferential CO oxidation process performed in a COPROX reactor is necessary in order to reduce CO concentration to appropriate levels for PEMFC applications. Conditions found in the present thermodynamic analysis pointed out that for ethanol reforming S/EtOH = 6 and 600°C will provide a HR of 5.7 and a hydrogen concentration as high as 97% with the use of a CO_2 absorbent (CaO). Otherwise, for the steam reforming of methanol optimal conditions found were S/MeOH = 4 and 600°C, which produced a hydrogen concentration of 98% using CaO as absorbent. Also, it is worth to mention that the thermal efficiency is closely related to the hydrogen concentration in the product gas as well as to the hydrogen production (HR). Therefore, these set of conditions also insure high thermal efficiencies for the AER process.

4.0 CONCLUSIONS

Thermodynamic analysis of steam reforming of light alcohols (ethanol and methanol) with and without CO_2 absorbents were carried out to determine favorable operating conditions to produce a high purity H_2 gas product.

Results indicate no carbon formation at steam to alcohol ratios less than stoichiometric values (S/COH ≤ stoichiometric) for the corresponding steam reforming reactions. However, for the ethanol system using CO_2 absorbents, carbon free operation can be found at S/EtOH ratios greater than 2.0 and temperatures higher than 958°C. While, for methanol reforming carbon free operation is achieved at steam/methanol ratios greater than 0.6 and temperatures higher than 778°C. Generally, carbon formation is suppressed with CO_2 absorption compared to conventional reforming operation for ethanol or methanol steam reforming.

The use of a CO_2 absorbent resulted in an increase in HR (mols H_2/mols alcohol) and H_2 purity. This enhancement under the ethanol reforming system produced a 19.2% increase in hydrogen production with respect to the conventional reforming and the hydrogen concentration was increased from 69 to 97%. Otherwise, with the methanol reforming system a 7% increase in hydrogen production was reached, while the hydrogen concentration increased from 73 to 98%. Under optimal operating conditions for AER process it is possible to produce a hydrogen concentration of ≈ 99% purity at 1 atm, 500°C and S/MeOH = 4 for methanol reforming, while this also can be achieved at 600°C and S/EtOH = 6 for ethanol reforming. For both alcohols CaO and CaO*MgO showed similar results with high levels of hydrogen production ratios and concentrations, Na_2ZrO_3 and Li_2ZrO_3 resulted only in slightly lower values than CaO, while Li_4SiO_4 showed significantly lower values than CaO. The order from higher to lower hydrogen production and concentration based on each CO_2 absorbent was as follows: CaO > CaO*MgO > Na_2ZrO_3 > Li_2ZrO_3 > Li_4SiO_4.

The thermal efficiency of the conventional reforming and AER systems were found to be strongly related to the hydrogen concentration in the product gas as well as to the hydrogen

production ratio (HR). The thermal efficiency was also enhanced with the use of a CO_2 absorbent since with the ethanol reforming system an increase from 66 to 81% was found with respect to the conventional process, while in the methanol reforming system the increase was from 67 to 77%.

The AER technology represents a promising low-temperature process for high-quality H_2 production with low propensity to carbon formation. Furthermore, the use of low temperatures could bring beneficial effects on the life of the catalysts and the construction materials of the reformers as well as in substantial energy savings. Besides these technological aspects, other advantages of the AER are expected, such as easy CO_2 sequestration. In this case, the use of alcohols in conjunction with AER could be a potentially viable carbon-negative process

Finally, Na_2ZrO_3 and Li_2ZrO_3 can be considered as promising alternate absorbents with comparable thermodynamics to the reference CaO absorbent for alcohol reforming applications in the present work. However, the limited durability of CaO and CaO*MgO absorbents make these zirconate materials ideal absorbents to be used under the AER system. However, from the two zirconates, Na_2ZrO_3 is the one that presents greater kinetics and superior stability. Therefore, Na_2ZrO_3 should be considered as a high potential absorbent under the AER of ethanol and/or methanol for future experimental evaluations.

5.0 REFERENCES

[1] N. A. Owen, O. R. Inderwildi and D. A. Kinga, *Energy Policy*, **38**, 4743-4749 (2010)

[2] S. Dunn, *Int J Hydrogen Energy,* **27**, 235-264 (2002)

[3] J. Schmidt, L. Sylvain, E. Dotzauer, G. Kindermann, E. Schmid, *Appl Energ*, **87**, 2128-2141 (2010)

[4] L. F. Brown, *Int. J. Hydrogen Energy*, **26**, 381-397 (2001)

[5] B. Amigun, J. Gorgens, H. Knoetze, *Energy Policy*, **38**, 312-322 (2010)

[6] A. I. Lysikov, S. N. Trukhan, A. G. Okunev, *Int J Hydrogen Energy*, **33**, 3061-3066 (2008)

[7] R. Davda, J. Shabaker, G. Huber, R. Cortright, J. Dumesic, *Appl Catal B: Environ*, **56**, 171-186 (2005)

[8] A. Lima da Silva, I. L. Müller, *Int J Hydrogen Energy*, **36**, 2057-2075 (2011)

[9] E. Ochoa-Fernández, H. Berntsen, T. Zhao, L. Hi, E. A. Blekkan, D. Chen, "CO_2 Sorption Enhanced Steam Reforming of Ethanol", North American Catalysis Society 20th North American Meeting , June 17-22, Abstract P-S12-34B (2007).

[10] N. Hildengrand, L. Readman, I. M. Dahl, R. Blom, *Appl. Catal., A,* **303**, 131-138 (2006)

[11] M. Kato, S. Yoshikawa, K. Nakawaga, *J. Mater Sci. Lett.*, **21**, 485 (2002).

[12] A. López, N. Pérez, A. Reyes, D. Lardizábal, *Sep. Sci. Technol.* **39**, 3563–3579 (2004)

[13] S. Jarungthammachote, A. Dutta, Energy Convers. Manage, **49**, 1345–1356 (2008).

[14] A. Roine, Chemical reaction and equilibrium software with extensive thermo-chemical database. Outokumpu HSC 6.0 Chemistry for windows 2010.

[15] M. Benito, J.L. Sanz, R. Isabel, R. Padilla, R. Arjona, L. Daza, *J Power Sources*, **151**, 11-17 (2005)

[16] A. N. Fatsikostas, X. E. Verykios. *J Catal*, **225**, 439-452 (2004)

[17] P. Biswas, D. Kunzru, *Int J Hydrogen Energy*, **32**, 969-980 (2007)

[18] L. He, J. M. S. Parra, E. A. Blekkan, D. Chen, *Energy Environ Sci*, **3**, 1046-1056 (2010)

[19] A. J. Akande, "Production of Hydrogen by Reforming of Crude Ethanol", Master of Science Thesis, University of Saskatchewan, Saskatoon, Saskatchewan, Canada (2005).

[20] M. Li, *Int J Hydrogen Energy*, **34**, 9362-9372 (2009)

[21] B. Zhang, X. Tang, Y. Li, W. Cai, Y. Xu, W. Shen, *Catal Commun*, **7**, 367-372 (2006)

[22] I. Fishtik , A. Alexander, R. Datta, *Int J Hydrogen Energy*, **25**, 31-45 (2000).

[23] M. Li, X. Wang, S. Li, S. Wang, X. Ma, *Int J Hydrogen Energy*, **35**, 6699-6708 (2010)

[24] L. P. R. Profeti, E. A. Ticianelli, E. M. Assaf, *Int J Hydrogen Energy*, **34**, 5049-60 (2009)

[25] L. He, H. Berntsen, E. Ochoa-Fernandez, J. C. Walmsley, E. A. Blekkan, D. Chen, *Top Catal*, **52**, 206-17 (2009).

[26] A. Lopez-Ortiz, D. P. Harrison, *Ind. Eng. Chem. Res.,* **40**, 5102 -5109 (2001)

[27] A. Silaban, D. P. Harrison, *Chem Eng Comm*, **47**, 149-162 (1996)

[28] C Han, D. P. Harrison, *Sep Sci Technol*, **32**, 681-697 (1997)

[29] A. Bandi, M. Specht, P. Sichler, N. Nicoloso, In situ gas conditioning in fuel reforming for hydrogen generation. 5th International Symposium on Gas Cleaning at High Temperature. Morgantown West Virginia. 2002. Available at: http://www.zsw-bw.de/en/docs/research/REG/pdfs/REG_5th_ISGC_2002.pdf.

[30] J. R. Hufton, S. Mayorga, S. Sircar, *AIChE Journal*, **45**, 248-256 (1999).

[31] Y. Ding, E. Alpay, *Process Saf Environ Prot*, **79**, 45-51(2001).

[32] K. Nakagawa, T. J. Ohashi, *J Electrochem Soc*, **145**, 1344-1346 (1998).

[33] M. Kato, S. Yoshikawa, K. Essaki, K. Nakagawa, Novel CO_2 absorbents using lithium-containing oxides. In Toshiba Corporation. INTERMAC, Japan Electric Measuring Instruments Manufacturers' Association, Joint Technical Conference.; **SE-3,** 1021 (2001).

[34] E. Ochoa-Fernández, C. Lacalle-Vilà, T. Zhao, M. Rønning, D. Chen, *Stud Surf Sci Catal*, **167**, 159-164 (2007).

[35] J. P. Jakobsen, E. Halmøy, *Energy Procedia*, **1**, 725-732 (2009).

[36] J. Papavasiliou, G. Avgouropoulos, T. Ioannides, *Catal Commun*, **6**, 497-501 (2005).

[37] B. A. Peppley, J. C. Amphlett, L. M. Kearns, R. F. Mann, *Appl Catal A: Gen*, **179**, 21-29 (1999).

[38] A. I. Lysikov, S. N. Trukhan, A. G. Okunev, *Int J Hydrogen Energy*, **33**, 3061-3066 (2008).

[39] M. Li, *Int J Hydrogen Energy*, **34**, 9362-9372 (2009).

[40] K. Faungnawakij, R. Kikuchi, K. Eguchi, *J Power Sources*, **161**, 87-94 (2006).